ELSEVIER

Intermetallics 9 (2001) 157–167

Intermetallics

www.elsevier.com/locate/intermet

Fabrication of Ni_3Al thin foil by cold-rolling

Masahiko Demura [a,*], Yozo Suga [b], Osamu Umezawa [a], Kyosuke Kishida [a], E.P. George [c], Toshiyuki Hirano [a]

[a] *National Research Institute for Metals, 1-2-1 Sengen, Tsukuba, Ibaraki 305-0047, Japan*
[b] *Nippon Cross Rolling Corporation, 697 Mobara, Mobara, Chiba 297-0026, Japan*
[c] *Metals and Ceramics Division, Oak Ridge National Laboratory, Oak Ridge, TN 37831-6093, USA*

Received 7 September 2000; received in revised form 13 October 2000; accepted 14 October 2000

Abstract

Thin foils of stoichiometric Ni_3Al with thicknesses ranging from 57 to 315 μm were successfully fabricated by heavily cold-rolling without intermediate annealing. Starting materials were produced by directional solidification using the floating zone method. The total reduction in thickness obtained was as much as 95.5%. This high rolling ductility is considered to be due to the monocrystalline or near monocrystalline form of the starting materials. X-ray pole figures showed the formation of {110} rolling texture. This {110} texture is considered to develop mainly as a result of compressive deformation normal to the rolling plane. The foils recrystallized at temperatures over 1273 K had some tensile ductility (3.0–14.6%) at room temperature in air, in contrast to the usual brittleness of polycrystalline Ni_3Al. Electron back scatter diffraction measurements revealed that low angle and Σ3 coincidence site lattice boundaries, which are considered to be crack-resistant, comprised 41–84% of the total grain boundary area in the recrystallized foils. This large fraction is probably a chief cause of the observed ductility. These results demonstrate that it may be possible to utilize Ni_3Al thin foils as lightweight, high-temperature structural materials, e.g. honeycomb structures. © 2001 Elsevier Science Ltd. All rights reserved.

Keywords: A. Nickel aluminides, based on Ni_3Al; B. Brittleness and ductility; B. Crystallographic texture; C. Recrystallization and recovery; C. Rolling

1. Introduction

Ni_3Al has attractive high-temperature properties such as anomalous strengthening with increasing temperature and excellent oxidation and corrosion resistance (see the review by Stoloff [1]). Considerable efforts have been made in recent decades to use this compound as a high-temperature structural material in bulk form [2]. In contrast to the bulk, if Ni_3Al thin foil were fabricated, lightweight structures, e.g. honeycomb structures, would be possible. They could then be used in high-performance engines.

At present, it is impossible to fabricate Ni_3Al foil on an engineering scale, e.g. by cold-rolling cast polycrystalline alloys, because of severe intergranular brittleness [3]. Aoki and Izumi discovered that microalloying with small amounts of boron improves ductility [4]. However, even with the addition of boron, ductility is not enough to cold-roll to thicknesses below 800 μm [2]. Another approach, twin roller casting from liquid metal, was tried, but it could not successfully produce foil [2,5]. Furthermore, this technique is not suitable for the fabrication of large-area foils. Thus, we think it is necessary to prepare a more ductile Ni_3Al which can be heavily cold-rolled.

In earlier studies, we found that directional solidification using the floating zone (FZ) method provides a significant ductility improvement for Ni_3Al without any boron additions [6,7]. Directionally solidified (DS) materials show high tensile elongation, more than 70% in ambient air, even though they have polycrystalline form with columnar-grained structure [8]. This ductility is larger than that of the boron-doped alloy, 53.8%, reported by Liu et al. [9]. The high ductility of the DS polycrystals was ascribed to the large fraction of low angle and low Σ-value coincidence site lattice boundaries in the columnar-grained structure [10]. Using the

* Corresponding author: Tel.: +81-298-59-2547; fax: +81-298-59-2501.
E-mail address: demura@nrim.go.jp (M. Demura).

0966-9795/01/$ - see front matter © 2001 Elsevier Science Ltd. All rights reserved.
PII: S0966-9795(00)00121-7

same technique we recently have succeeded in growing single crystals of stoichiometric Ni_3Al [11,12], which has previously been considered difficult, if not impossible. As is well known, monocrystalline Ni_3Al has substantial ductility, more than 100% elongation [3]. Taking advantage of the high ductility of these DS materials, we fabricated thin foil by cold-rolling in this study.

The purpose of this paper is to present the details of the cold-rolling process. Another purpose is to report the ductility of recrystallized foil in air at room temperature. This is because the loss of ductility due to recrystallization is of great concern for structural applications. Cold-worked Ni_3Al recrystallizes at high temperatures and forms equiaxed grains which are similar to the cast and homogenized alloys. As is well known, these alloys are very brittle in the absence of boron [9,13]. They fracture at grain boundaries just after yielding, mostly due to the presence of moisture in air [14,15]. Thus, we present here the recrystallized microstructures of the foils and the room-temperature tensile properties in air.

2. Experimental

Three rods, designated as nos. 31–2, 41-1, and 42-2, of boron-free binary stoichiometric Ni_3Al were grown by the FZ method in an image furnace with double halogen lamps at a growth rate of 25 mm/h. The feed rod preparation and crystal growth procedure were previously described [6]. In order to obtain high single crystallinity, the crystal diameter was kept constant during the crystal growth by controlling the power of the lamps. On average the grown rods were 12 mm in diameter and 150 mm in length. Table 1 summarizes the Al contents of the three rods as determined by inductively coupled plasma spectroscopy. The Al contents are close to the stoichiometric composition (25 at.% Al).

The grown rods were sectioned into sheets along the growth direction by electric discharge machining. Their surfaces were mechanically polished. The optical microstructures were examined by etching with Marble reagent (2.5 g $CuSO_4$, 30 cm^3 HCl, and 25 cm^3 H_2O). Sample no. 31-2 was mostly single crystal but contained columnar grains with low angle boundaries in places. Samples nos. 41-1 and 42-2 were single crystals. The initial rolling direction (or growth direction) and rolling plane of the sheets were determined by the Laue X-ray back reflection method as summarized in Table 1.

First, the sheets (about 1 or 2 mm in initial thickness; see Table 2) were cold-rolled to about 300 μm in thickness by

Table 1
Analyzed Al contents and initial orientation (rolling plane and direction)

Sample	Al content	Initial orientation	
no.	(at.%)	Rolling plane	Rolling direction
31-2	24.4	{0.2 0.1 1.0}	⟨1.0 0.0 0.2⟩
41-1	24.7	{3.9 1.0 5.2}	⟨4.0 9.0 4.8⟩
42-2	24.8	{2.0 1.0 4.3}	⟨1.1 2.0 1.0⟩

Table 2
Results of cold rolling: thickness of the sheet before and after cold rolling, reduction in thickness, and rolling texture

Sample	Thickness (μm)		Reduction	
no.	Before rolling	After rolling[a]	(%)	Rolling texture
31-2	959	315 (28)	67	–[b]
		73 (1)	92	{110}–⟨113⟩ + {110}⟨117⟩
		57 (2)	94	–[b]
41-1	2043	91 (0)	95.5	{110}⟨113⟩
42-2	1917	307 (18)	84	{110}⟨113⟩

[a] The number in parentheses represents fluctuation in thickness in the rolling direction.
[b] Not measured.

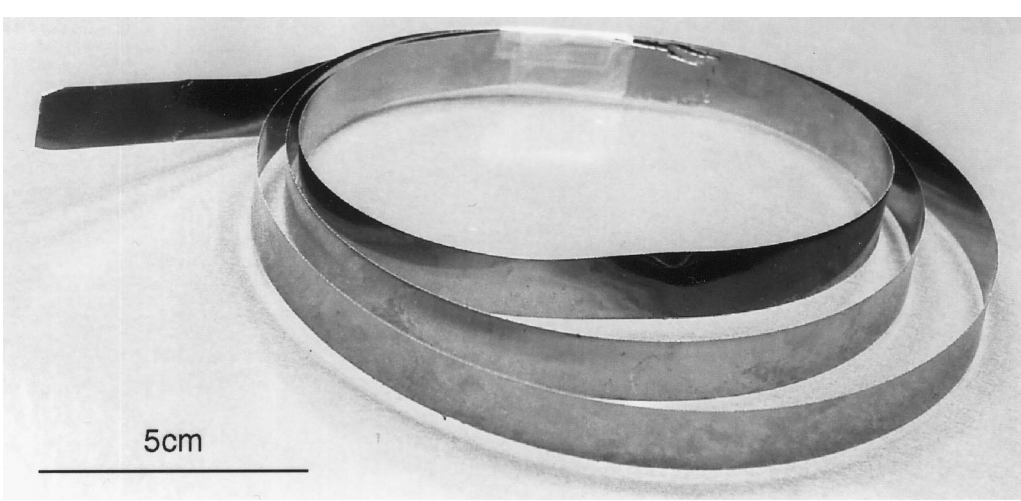

Fig. 1. 91 μm-thick, 10 mm-wide and about 1 m-long foil of sample no. 41-1 cold-rolled to 95.5% reduction in thickness.

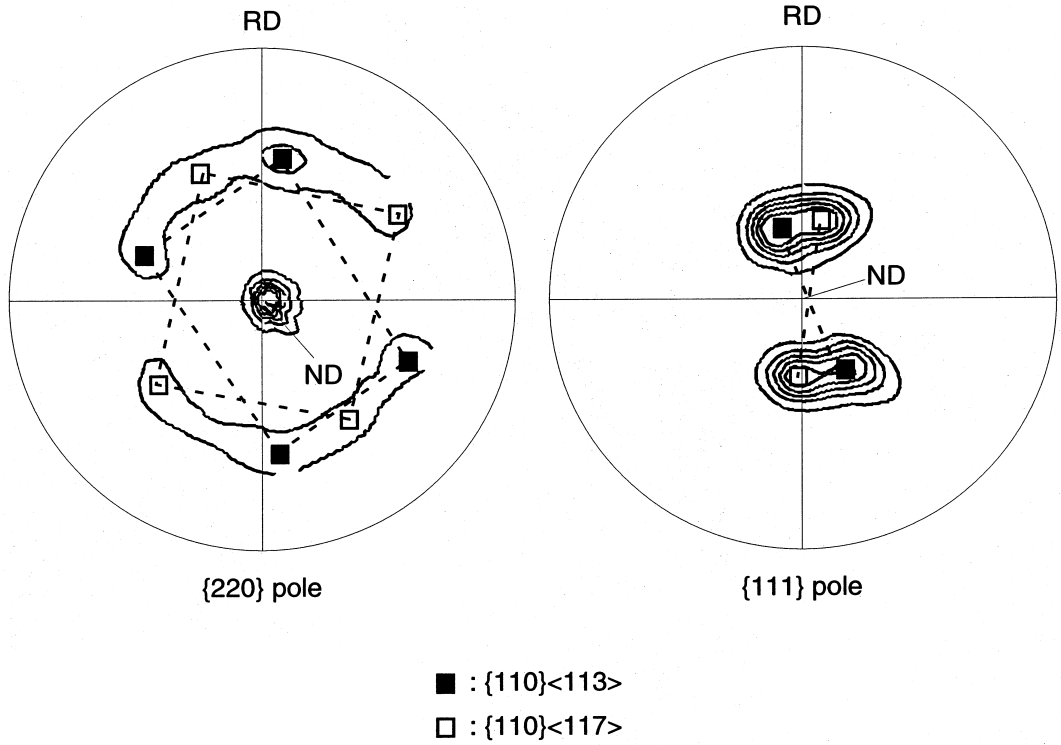

Fig. 2. The rolling texture of 73 μm-thick foil of sample no. 31-2 after cold-rolling (92% reduction): (a) {220} and (b) {111} pole figures. Open and solid squares represent {110} ⟨117⟩ and {110}⟨113⟩ textures, respectively.

using four-high mills with a work roll diameter of 110 mm. Then, they were rolled further using cemented carbide rolls having a roll diameter of 75 mm. Both the cold-rolling operations were performed without intermediate annealing or lubricant. The rolling textures of the foils were measured by X-ray Schultz back reflection method.

The tensile properties of the recrystallized foils were studied using two foils of sample no. 31-2 with two different thicknesses: 73 μm-thick foil (92% reduction) and 315 μm-thick foil (67% reduction). These foils were recrystallized at temperatures between 1273 and 1573 K for 1.8 ks in a vacuum better than 1×10^{-4} Pa. The optical microstructures were examined by etching with Marble reagent. The average grain size was measured by the line intercept method without correction. The orientation of the recrystallized grains was measured at 1 or 5 μm scanning steps by electron back scatter diffraction (EBSD) in a scanning electron microscope (SEM). The grain boundary (GB) character, or Σ-value, was calculated based on Brandon's criterion [16]: if the deviation angle from an exact coincidence site lattice (CSL) relation is less than $15°/\sqrt{\Sigma}$, the boundary is referred to as a CSL boundary with that Σ-value. The maximum Σ-value was set as 25 (i.e. those with higher Σ-values were designated as random boundaries). The area fraction of each GB type was two-dimensionally evaluated by measuring GB length in the EBSD-SEM image, instead of the number fraction.

Tensile specimens with gauge length of 10 mm were cut from the recrystallized foils by electric discharge machining. The gauge widths were 3 mm and 5 mm for 73 and 315 μm-thick foils, respectively. Tensile tests were performed at room temperature in air at a strain-rate of 8×10^{-4} s^{-1}. The load data were collected at a frequency of 5 Hz with a computer and the true stress was calculated by assuming uniform deformation: no obvious necking was observed during testing. The strain was calibrated by measuring the change in gauge length

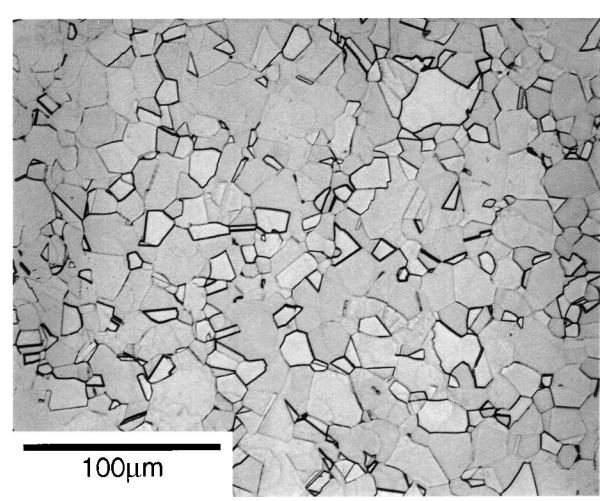

Fig. 3. Microstructure of 73 μm-thick foil of sample no. 31-2 recrystallized at 1273 K for 1.8 ks.

after the tests, assuming a constant strain rate. The fracture surface was examined by SEM.

3. Results

3.1. Cold-rolling

It was possible to cold-roll the starting sheets to thin foil less than 100 μm in thickness without intermediate annealing. Fig. 1 shows a 1 m long foil of sample no. 41-1 that is 91 μm thick and 10 mm wide. In this case the total reduction in thickness amounts to 95.5%. The surface is crack-free and smooth, with little fluctuation in thickness along the rolling direction. With a shiny metallic luster, it looks like a mirror. The foil is heavily work-hardened, with a Vickers hardness of about 620, but it is nevertheless possible to make a coil, as shown in Fig. 1. Also, the foil is ductile and could be bent plastically; hence honeycomb structures may be possible. It is worth noting that such high-quality thin foil was fabricated by cold-rolling boron-free, binary NiAl, which is considered a brittle intermetallic compound.

Similarly high rolling ductility was obtained in other samples, nos. 31-2 and 42-2, which had different initial orientations (Table 1). The results are summarized in Table 2. Samples nos. 41-1 and 42-2 are single crystals, and hence the results may be somewhat expected because Ni_3Al is known to be ductile in a single crystal form [3]. In the case of binary, stoichiometric alloys, the problem is the difficulty in growing single crystal [12]. Sample no. 31-2 had some columnar grains, but this did not hinder cold-rolling. As we previously reported [7], the columnar-grained polycrystals grown by the FZ method are ductile because most of the boundaries are low-angle and low-Σ types [10].

The {220} and {111} pole figures of the 73 μm-thick foil of sample no. 31-2 are shown in Fig. 2 (a) and (b), respectively. The {220} pole has the highest intensity peak at the normal direction (ND) and surrounding high intensity regions about 60 degrees away from the ND. The {111} pole has two high intensity peaks, which are slightly split, at points about 35° away from the ND toward the rolling direction (RD). These pole figures imply that the foil consists of {110} ⟨113⟩ and {110} ⟨117⟩ textures.

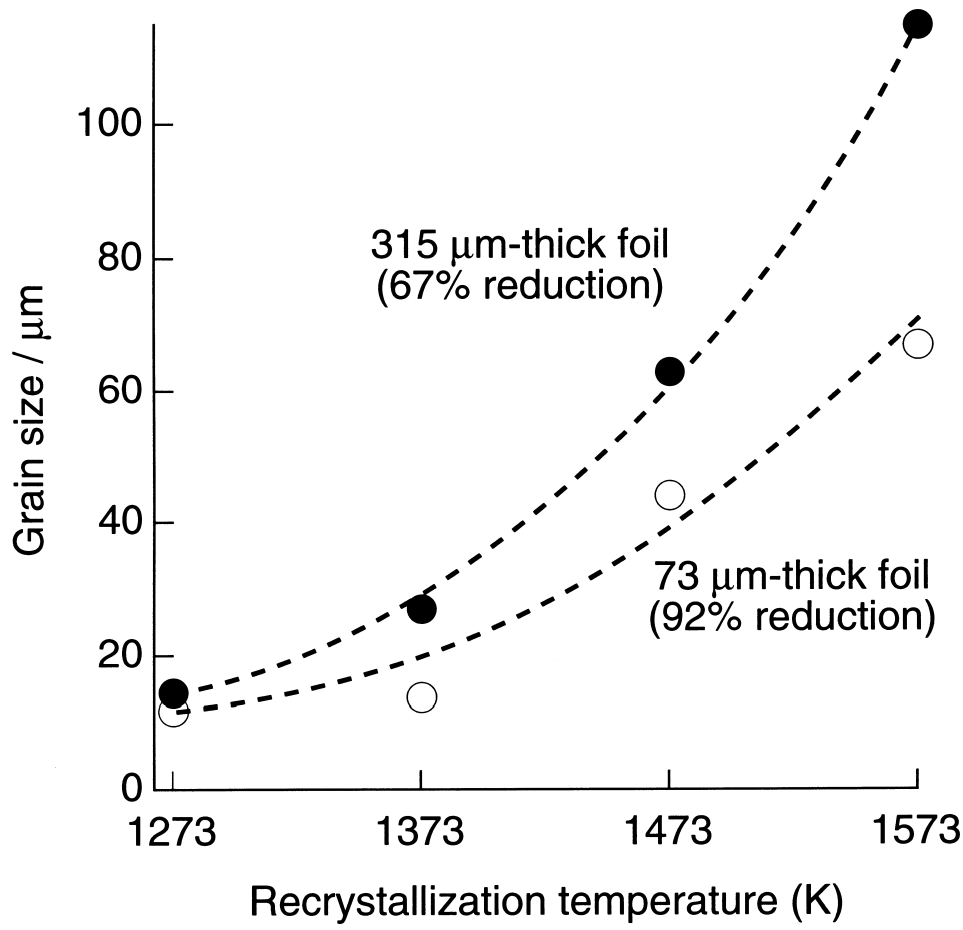

Fig. 4. Average grain size as a function of recrystallization temperature for 73 μm- (92% reduction) and 315 μm-thick foil (67% reduction) of sample no. 31-2.

Table 2 summarizes the rolling textures observed. There is some difference among the samples. Samples nos. 41-1 and 42-2 possess a single {110} ⟨113⟩ texture, unlike no. 31-2. However, note that even with this minor difference the rolling plane {110} is the same. This {110} texture may be related to the high reduction of cold-rolling. Probably, the RD depends on the initial orientation of the sheet, but the details are not known.

3.2. Recrystallization

It has been reported that the recrystallization of Ni_3Al starts between 900 and 1000 K, depending on the amount of rolling reduction [17]. Consistent with this, both 73 and 315 μm-thick foils of sample no. 31-2 were fully recrystallized above 1273 K. Fig. 3 is an optical micrograph of the 73 μm-thick foil heat-treated at 1273 K for 1.8 ks. It shows a typical recrystallized microstructure which consists of equiaxed grains with homogeneous grain size. A similar grain morphology was observed in the foils heat-treated above 1273 K and also in the 315 μm-thick foils. Fig. 4 plots the average grain size as a function of heat treatment temperature. The grain size increases with increasing heat treatment temperature. The 73 μm-thick foils have smaller grain size than the 315 μm-thick foils. This is probably related to the difference in the amounts of cold reduction. The greater the reduction, the larger the amount of strain energy that is stored, which enhances the nucleation of recrystallization, leading to the finer grain.

Fig. 5 shows the area fraction of GB types in the 73 and 315 μm-thick foils of sample no. 31-2 recrystallized at 1273 and 1573 K. The recrystallized foils consist mostly of three types of boundaries: low angle (LAB), Σ 3 and random boundaries (RB). Very small amounts of CSL boundaries between Σ5 and 25 exist in the foils

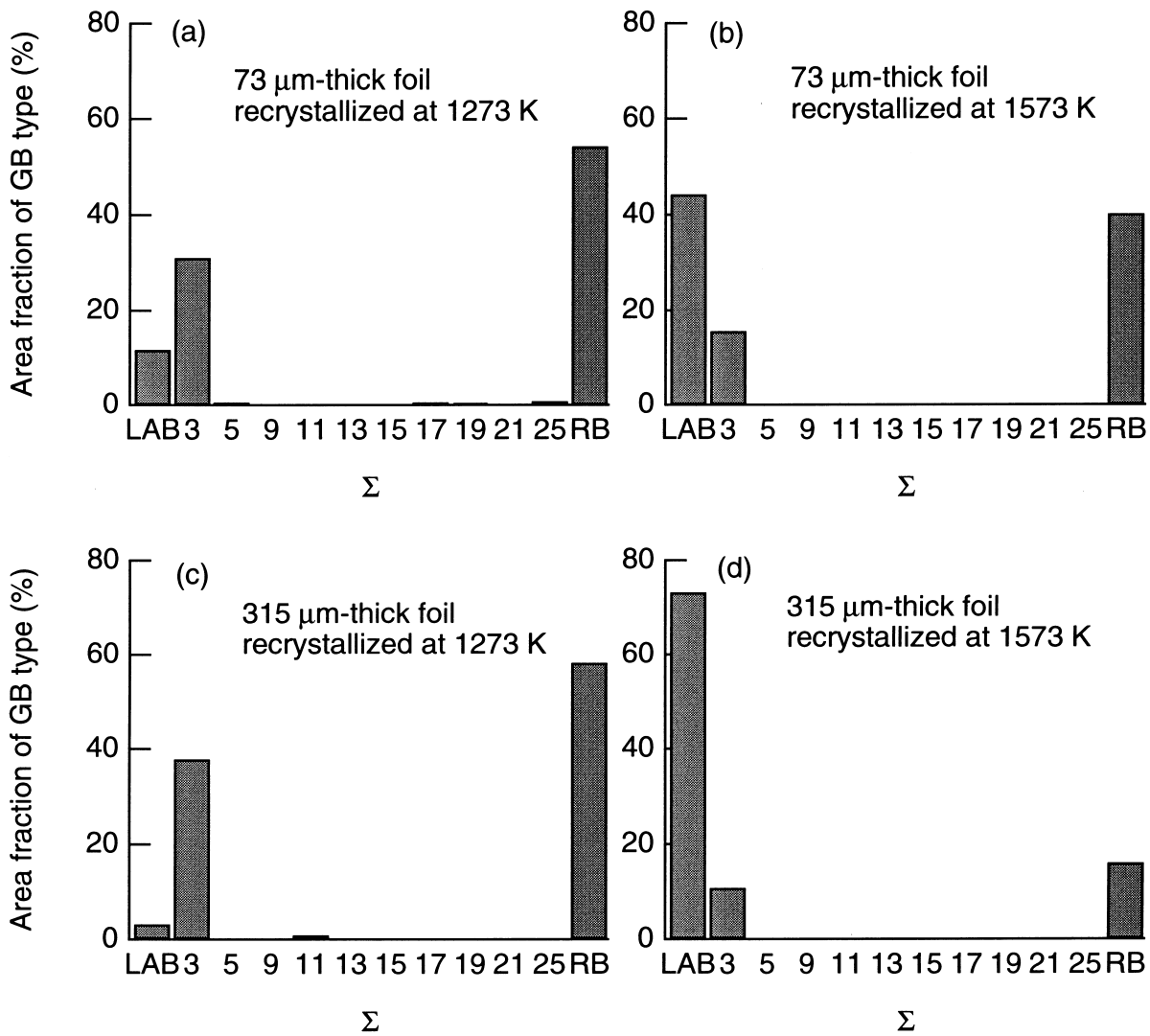

Fig. 5. Area fraction of CSL boundaries between Σ 1 (low angle boundary, LAB) and Σ 25, and random boundaries (RB) in the recrystallized foils of sample no. 31–2: (a) 73 μm-thick, recrystallized at 1273 K, (b) 73 μm-thick, recrystallized at 1573 K, (c) 315 μm-thick, recrystallized at 1273 K and (d) 315 μm-thick, recrystallized at 1573 K.

recrystallized at 1273 K. Table 3 summarizes the area fraction of each GB type. Note that the foils have a large fraction of LAB and Σ3 boundaries which are considered to be crack-resistant [18,19]. There is a tendency that as the heat treatment temperature increases, the total fraction of LAB and Σ3 increases, and the fraction of RB, which is considered to be very susceptible to cracking, decreases. It is generally believed that low energy boundaries, LAB and Σ3, migrate slowly, while high energy boundaries, high Σ and RB, migrate faster. From Fig. 5 and Table 3, it is likely that grain growth occurs mainly by the migration of high Σ and RB, resulting in the observed high fractions of LAB and Σ3.

3.3. Tensile properties of the recrystallized foils

Fig. 6 shows the room-temperature stress-strain curves of 73 and 315 μm-thick foils of sample no. 31-2 recrystallized at various temperatures. Note that all the foils show some ductility after yielding. The foils recrystallized at 1573 K show the highest ductility: 5.6 and 14% elongations for 73 and 315 μm-thick foils, respectively. Though the ductility decreases with decreasing recrystallization temperature, the foils recrystallized at 1273 K still show 3% elongation. With this elongation, it is possible to bend more than 100° as shown in Fig. 7, probably because of the thinness of the foils. Thus, the ductility loss due to recrystallization is not a serious problem in our foils. These ductilities normally cannot be expected for boron-free polycrystalline Ni_3Al. As expected, the yield stress decreases with increasing recrystallization temperature, owing to the increase in grain size.

Fig. 8 shows the fracture surfaces of the recrystallized foils after the above tensile tests. Intergranular fracture is dominant in both the 73 and 315 μm-thick foils recrystallized at 1273 K, while the fraction of transgranular fracture is rather high in the foils recrystallized at

Table 3
Area fraction of grain boundary types in the recrystallized foils of no. 31-2

Thickness	Heat treatment	Area fraction (%)				
(μm)	temperature (K)	LAB	Σ 3	LAB + Σ 3	Σ 5-25	RB
73	1273	11.7	31.0	42.7	3.1	54.2
73	1573	44.3	15.6	59.9	0	40.1
315	1273	3.2	37.8	41.0	0.8	58.2
315	1573	73.2	10.8	84.0	0	16.0

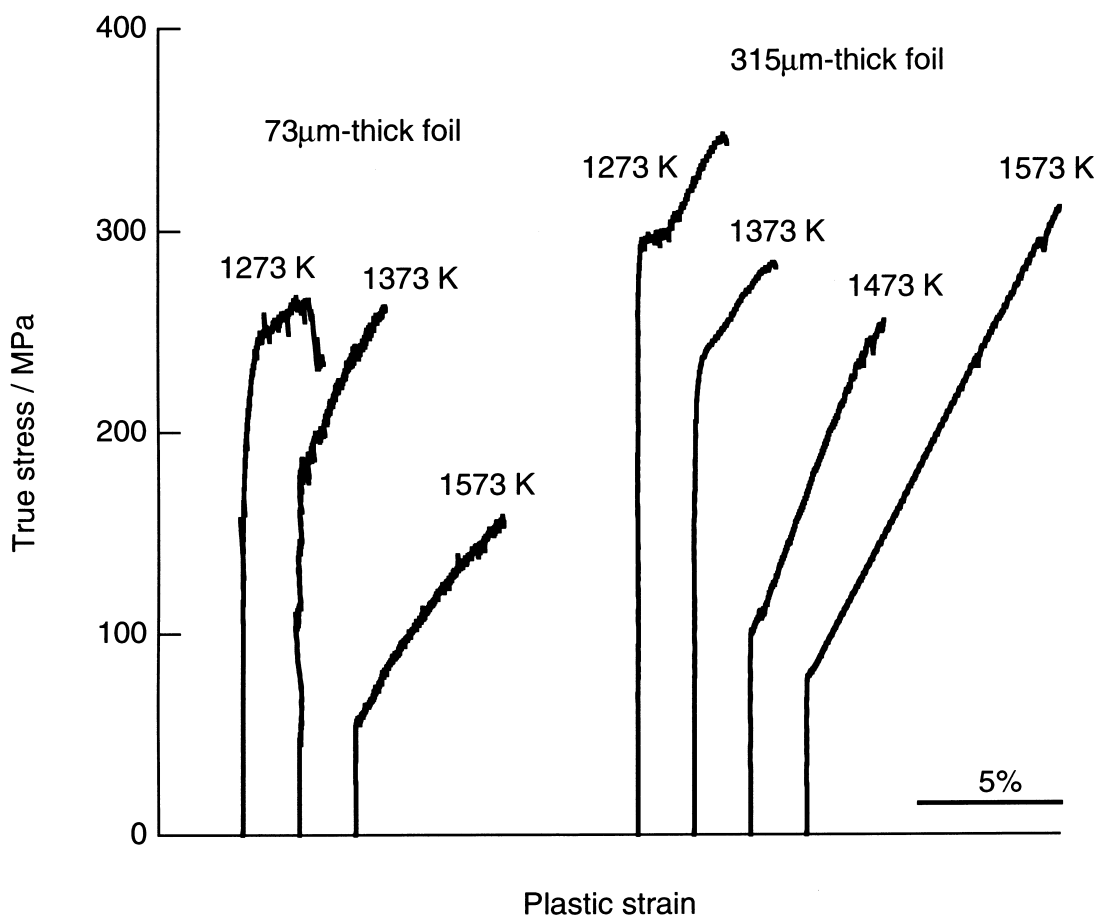

Fig. 6. Stress–strain curves for the recrystallized foils of sample no. 31-2: 73 and 315 μm-thick foils.

1573 K. The change in fracture mode correlates well with both the ductility (Fig. 6) and the fraction of the LAB and Σ3 boundaries (Table 3). It is therefore concluded that with increasing heat treatment temperature, the fraction of the crack-resistant boundaries, LAB and Σ3, increases, resulting in high ductility by suppressing intergranular fracture.

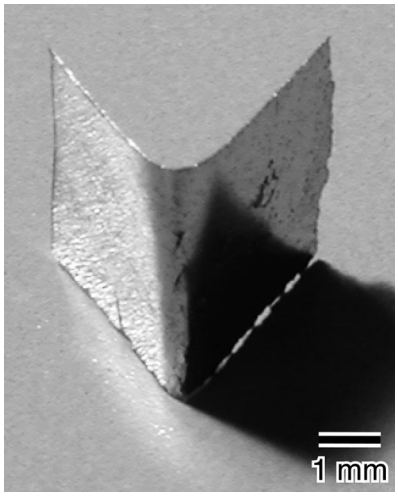

Fig. 7. Photograph of 73 μm-thick foil of sample no. 31-2 recrystallized at 1273 K, showing bending of more than 100°.

In thin foils, the number of grains across the thickness is limited, unlike in bulk samples. Particularly in the thinner 73 μm-thick foils recrystallized at 1573 K, the grain diameter is comparable to the foil thickness, producing a near bamboo structure. Note that this specimen exhibited 5.6% elongation (Fig. 6), though some cracks propagated along a single boundary from one surface to the other, as shown in Fig. 9. Intergranular fracture is therefore suppressed to some extent, even in those boundaries that do finally fracture.

4. Discussion

This is the first report of successful fabrication of thin foils of Ni_3Al less than 100 μm in thickness. The reason for this success is mainly that our starting materials were monocrystalline or near monocrystalline alloys grown by controlled directional solidification. We will now discuss the deformation during cold-rolling and the mechanical properties of the recrystallized foils.

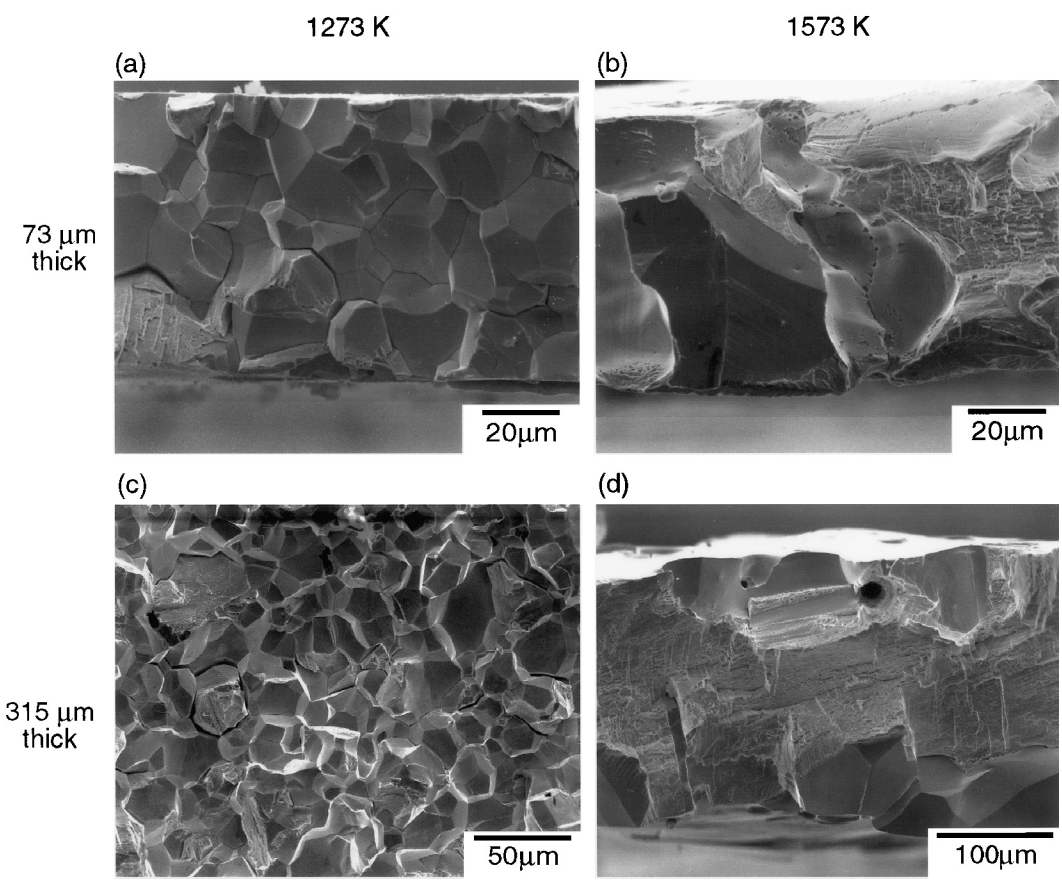

Fig. 8. Fracture surfaces of the recrystallized foils of sample no. 31-2: (a) 73 μm–thick foil recrystallized at 1273 K, (b) 73 μm-thick at 1573 K, (c) 315 μm-thick at 1273 K, and (d) 315 μm-thick at 1573 K.

4.1. Deformation during cold-rolling

It is likely that the observed {110} texture is a characteristic of the high thickness reduction of Ni_3Al alloys. Table 4 lists the previously observed rolling textures in Ni_3Al. Escher et al. found the same {110}⟨113⟩ rolling texture in a 80% cold-rolled Ni-rich Ni_3Al single crystal [20] as we did. In addition, two groups reported the rolling texture developed in boron-doped ductile polycrystalline alloys. Gottstein et al. reported a mixture of mainly two {110} textures with different rolling directions after cold reduction of 90% [17]. Chowdhury found {110} texture with weak {112} and {123} textures after cold reduction of 85% [21]. From this comparison, the {110} texture seems to be common in Ni_3Al cold-rolled over 80%, irrespective of crystal forms and whether or not the alloy is doped with boron.

The {110} texture can be understood in terms of compressive deformation normal to the rolling plane, as follows. In compression a crystal changes its orientation so that the normal direction to the slip plane approaches the compressive direction, a process known as lattice rotation. The slip system of Ni_3Al is {111} ⟨110⟩ at room temperature [22], similar to that of fcc metals, e.g. Cu and Al. Let us suppose the case of a single crystal with ND shown in Fig. 10. When it is compressed along the ND, primary (111)[101] slip is activated and the ND rotates toward the (111) pole, as shown by the arrow '1'. When the ND crosses the (100) great circle, conjugate (111)[101] slip starts to operate. This causes the ND to rotate toward the (111) pole, as shown by the arrow '2'. When both the primary and conjugate slip systems operate equally, the ND finally reaches the stable orientation, i.e. the (011) pole. We consider that this idea can explain qualitatively the evolution of {110} texture in our DS materials, since they have monocrystalline or near monocrystalline forms.

Gottstein et al. reported that cold-rolling often caused premature cracking in their boron-doped polycrystalline Ni_3Al [17]. On the contrary, our DS sheets could reach

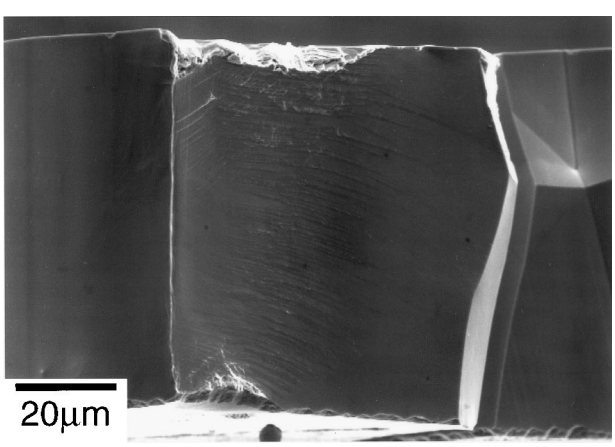

Fig. 9. Fracture surface of 73 μm-thick foil of sample no. 31-2 recrystallized at 1573 K, showing an intergranular fracture of partial bamboo structure.

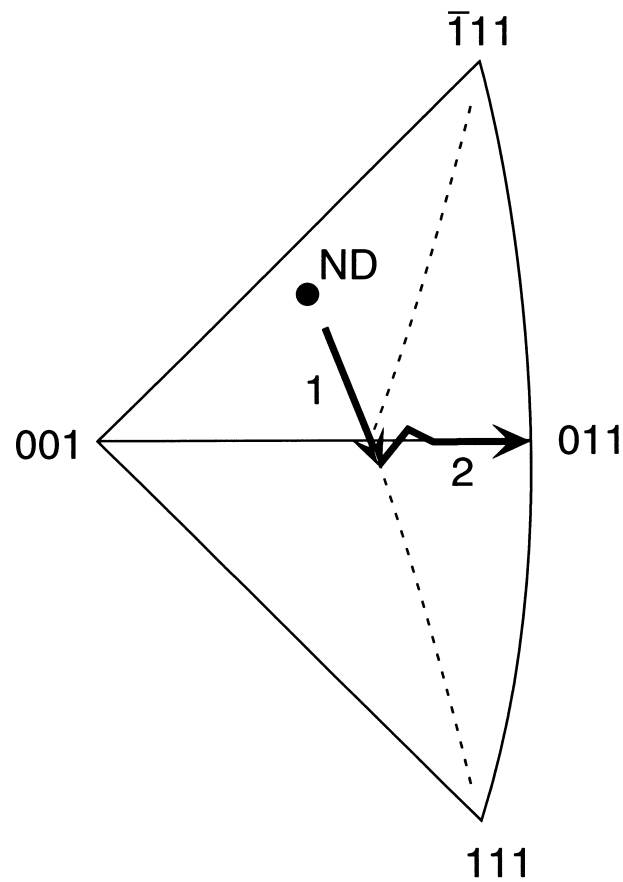

Fig. 10. A schematic illustration of the lattice rotation of Ni_3Al single crystal by compressive stress normal to the rolling plane (ND) during cold-rolling. First, the ND rotates along the arrow '1' by operation of (111)[101] primary slip and then toward (011) along the arrow '2' by operation of the primary and (111)[101] conjugate slip.

Table 4
Summary of previous results on the rolling texture of single crystal and polycrystalline Ni_3Al

Alloy	Crystal form	Reduction (%)	Texture	Ref.
Ni–24 at.% Al with and without B	Single crystal {617}293[a]	80	{110}⟨113⟩	[20]
Ni–24 at.% Al – 0.24 at.% B	Polycrystal	90	Mixture of {110} ⟨112⟩ and {110} ⟨100⟩	[17]
Ni–24 at.% Al – 0.24 at.% B	Polycrystal	85	Mixture of {110}⟨112⟩ {112}⟨111⟩ and {123}⟨634⟩	[21]

[a] The initial rolling plane and direction.

the {110} stable orientation without any cracks, showing high reduction up to 94% even in near monocrystalline form with columnar grains (i.e. Sample no. 31-2). As described in Section 3.1, this high performance in cold-rolling may be related to the fact that grain boundaries in our DS materials are low angle and low Σ types. That is, it can be concluded that these boundaries are strong enough to withstand the stresses generated at the grain boundaries during the rolling deformation of individual grains. In other words, other boundaries such as high Σ and random boundaries probably hinder cold-rolling in polycrystalline Ni_3Al, and this problem may be too difficult to be overcome by boron-doping. At present, however, the detailed process of rolling deformation has yet to be clarified.

4.2. Mechanical properties of recrystallized foil

4.2.1. Ductility

Our recrystallized foils possess good ductility in air (Figs. 6 and 7), which is a significant advantage in structural applications. As described in Section 3.3, this ductility is mainly due to the high fraction of LAB and Σ3 boundaries. Hanada et al. found no cracks along these boundaries in bent specimens of recrystallized, stoichiometric Ni_3Al [18], suggesting higher crack-resistance compared to other boundaries. This was confirmed by Lin and Pope, who examined the distribution of cracked boundaries as a function of Σ-value in bent specimens of melt-spun Ni_3(Al, 0.2 at.% Ta) ribbons [19]. These previous works were qualitative evaluations of the fracture strength of each boundary, but very recently, we found that these LAB and Σ3 boundaries do not fracture in air when bicrystal specimens were uniaxially tensile tested [23]. This new finding shows that the fracture strength of these two types of boundaries is comparable to that of single crystals. Thus, the presence of these two types of boundaries enhances the overall ductility of Ni_3Al, though a quantitative relation between their fraction and ductility is still not obtained.

To date, ductilities ranging from 3 to 15% elongation were reported in recrystallized boron-free Ni_3Al

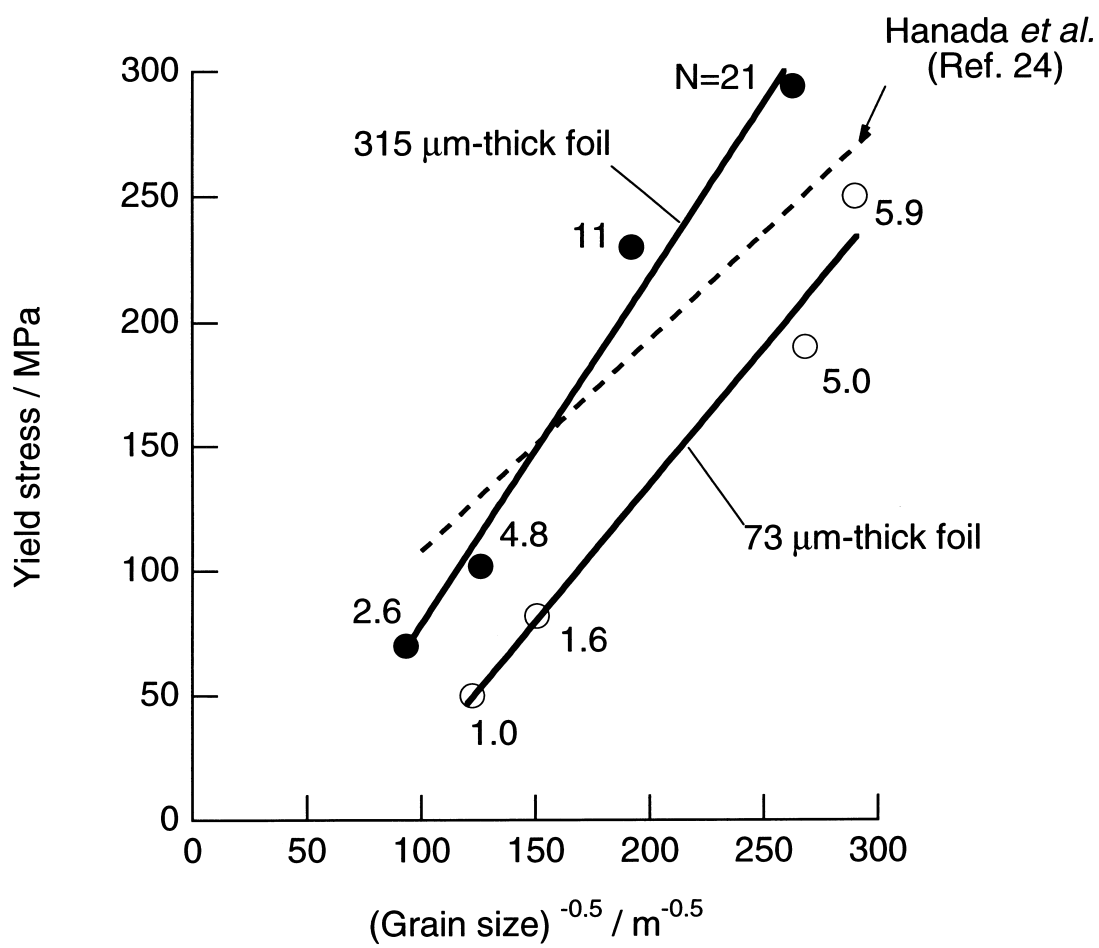

Fig. 11. Yield stress as a function of the inverse of the square root of grain size in 73 μm- (open circle) and 315 μm-thick (solid circle) foils of sample no. 31-2 recrystallized at temperatures higher than 1273 K foils. Numbers adjacent to the data points show the numbers of grains across the foil thickness, which is calculated by dividing the thickness by the grain size. Dashed line represents the results of recrystallized Ni_3Al sheet (1.5 mm in thickness) reported by Hanada et al. [24].

[13,15,18,24–26], in contrast to almost no elongation in cast and homogenized alloys [9,13]. There is a tendency that the ductility increases with deviation to the Ni-rich side from the stoichiometric composition [24,25]. However, 5–7% elongation has been reported in some stoichiometric alloys [18,24]. The fabrication technique, casting and cold-rolling, is likely the key to improving ductility in polycrystalline Ni_3Al. It is usually difficult to cold-roll Ni_3Al, but once this barrier is cleared, the recrystallized alloys can possess some tensile ductility. We believe that in our case the key is directional solidification, which allows heavy cold reductions accompanied by strong texture evolution. This strong rolling texture in turn may result in high fractions of LAB and $\Sigma 3$ boundaries in the recrystallized foils.

In thin foils having a small number of grains across the thickness, there is a possibility that all the grain boundaries from one surface to the other are weak, i.e. high Σ or random types. This weak-boundary linkage is considered to control the ductility, especially in bamboo-structured foil, since cracks propagate without being hindered by other grains, and thus the ductility is controlled by the single weakest boundary. This is the case shown in Fig. 9. From the observed intergranular fracture mode, it is concluded that the fractured boundary was probably neither LAB nor $\Sigma 3$ boundary [23]. Nevertheless, the foils showed some elongation. This means that boundaries other than LAB and $\Sigma 3$ can resist cracking to some extent. That is, our recrystallized foils possess at least 3% tensile elongation, irrespective of grain boundary types.

4.2.2. Yield stress

Fig. 11 shows a Hall–Petch plot of the yield stress. The yield stress increases with decreasing grain size for both 73 and 315 μm-thick foils, showing that the grain boundaries are obstacles to dislocation motion as in conventional metals. In this regard, our thin foils are not different from bulk material, e.g. recrystallized 1.5 mm thick sheets reported by Hanada et al. [24] (the dashed line in Fig. 11).

However, the thinner 73 μm-thick foils show lower yield stress than the 315 μm-thick foils as shown in Fig. 11. Also, the two slopes are different from each other: 1.10 and 1.39 MPa $m^{1/2}$ for 73 and 315 μm-thick foils, respectively. Thus, the Hall-Petch relation does not strictly hold in the recrystallized foils. The lower yield stress of the 73 μm-thick foil should probably be ascribed to the smaller number of grains across the foil thickness. The number of grains, N, shown in Fig. 11, is very small, particularly for the thinner 73 mm-thick foil. Miyazaki et al. [27] reported that yield stress decreases with decreasing N if N is less than a critical value ranging from 5 to 20, because constraint by neighboring grains becomes weak. Perhaps this effect was observed in our foils.

5. Conclusion

Thin foils of stoichiometric Ni_3Al below 100 μm in thickness with crack free and smooth surfaces were fabricated by cold-rolling without intermediate annealing. Starting sheets, which were sectioned from rods directionally solidified by using the floating zone method, were single crystals or nearly single crystals with a few columnar grains.

In all the sheets, high rolling ductility was observed: reductions in thickness over 84% could be obtained, irrespective of the initial orientation and existence of columnar grains. The rolled foils had {110} textures, irrespective of initial rolling direction and plane. The observed texture is considered to be the result of the operation of two {111} ⟨101⟩ slips by compressive stress normal to the rolling plane.

The foils recrystallized at temperatures between 1273 and 1573 K for 1.8 ks had some ductility, 3–14.6%, in contrast to cast, polycrystalline Ni_3Al which normally shows almost no elongation. The ductility was mainly related to the area fraction of low angle and $\Sigma 3$ coincidence site lattice boundaries, which ranged from 41 to 84% depending on the heat treatment temperature. These boundaries are considered to be more crack-resistant than other boundaries, i.e. high Σ and random types. The yield stress increased with decreasing grain size, but the Hall–Petch relation did not hold exactly.

Acknowledgements

This research was supported partially by the Division of Materials Science and Engineering at the Oak Ridge National Laboratory, managed by UT-Battelle, LLC, for the US Department of Energy under contract DE-AC05-00OR22725.

References

[1] Stoloff NS. Int Mater Rev 1989;34:153.
[2] Liu CT, Sikka VK. J Metals 1986;38:19.
[3] Aoki K, Izumi O. Trans JIM 1978;19:203.
[4] Aoki K, Izumi O. Nihon Kinzoku Gakkai Shi 1979;43:1190.
[5] Taub AI, Huang SC, Chang KM. Metall Trans A 1984;15A:399.
[6] Hirano T. Acta Metall Mater 1990;38:2667.
[7] Hirano T. Scripta Metall Mater 1991;25:1747.
[8] Hirano T, Kainuma T. ISIJ International 1991;31:1134.
[9] Liu CT, White CL, Horton JA. Acta Metall 1985;33:213.
[10] Watanabe T, Hirano T, Ochiai T, Oikawa H. Materials Science Forum 1994;157-162:1103.
[11] Demura M, Hirano T. Phil Mag Letters 1997;75:143.
[12] Golberg D, Demura M, Hirano TJ. Crys Growth 1998;186:624.
[13] Aoki K, Izumi O. Trans JIM 1978;19:145.
[14] George EP, Liu CT, Pope DP. Scripta Metall Mater 1992;27:365.
[15] George EP, Liu CT, Pope DP. Scripta Metall Mater 1993;28:857.

[16] Brandon DG. Acta Metall 1966;14:1479.
[17] Gottstein G, Nagpal P, Kim W. Mater Sci Eng A 1989;108:165.
[18] Hanada S, Ogura T, Watanabe S, Izumi O, Masumoto T. Acta Metall 1986;34:13.
[19] Lin H, Pope DP. Acta Metall Mater 1993;41:553.
[20] Escher C, Neves S, Gottstein G. Acta Mater 1998;46:441.
[21] Chowdhury SG, Ray RK, Jena AK. Scripta Metall Mater 1995;32:213.
[22] Thornton PH, Davies RG, Johnston TL. Metall Trans 1970;1:207.
[23] Su JQ, Demura M, Hirano T. Unpublished data.
[24] Hanada S, Watanabe S, Izumi OJ. Mater Science 1986;21:203.
[25] Chiba A, Hanada S, Watanabe S, Obana T, Tanosaki K, Fujita M. Mater Trans JIM 1992;33:503.
[26] Chiba A, Hanada S, Watanabe S, Abe T, Obana T. Acta Metall Mater 1992;42:1733.
[27] Miyazaki S, Shibata K, Fujita H. Acta Metall 1979;27:855.